Published in final edited form as:
J Pathol. 2011 October ; 225(2): 212–221. doi:10.1002/path.2929.

Orthotopic xenografts of RCC retain histological, immunophenotypic and genetic features of tumors in patients

Chiara Grisanzio[1,2], **Apryle Seeley**[1,2], **Michelle Chang**[1], **Michael Collins**[1], **Arianna Di Napoli**[1], **Su-Chun Cheng**[3], **Andrew Percy**[4], **Rameen Beroukhim**[2,5], and **Sabina Signoretti**[1,2]

[1]Department of Pathology, Brigham and Women's Hospital, Harvard Medical School, Boston, MA, 02115, USA

[2]Department of Medical Oncology, Harvard Medical School, Boston, MA, 02115, USA

[3]Department of Biostatistics and Computational Biology, Dana-Farber Cancer Institute, Harvard Medical School, Boston, MA, 02115, USA

[4]Division of Hematology/Oncology, Beth Israel Deaconess Medical Center, Harvard Medical School, Boston, MA, 02115, USA

[5]Broad Institute of MIT and Harvard, Cambridge, MA 02142, USA

Abstract

Renal cell carcinoma (RCC) is an aggressive malignancy with limited responsiveness to existing treatments. *In vivo* models of human cancer, including RCC, are critical for developing more effective therapies. Unfortunately, current RCC models do not accurately represent relevant properties of the human disease.

The goal of this study was to develop clinically relevant animal models of RCC for preclinical investigations. We transplanted intact human tumor tissue fragments orthotopically in immunodeficient mice. The xenografts were validated by comparing the morphologic, phenotypic, and genetic characteristics of the kidney tumor tissues before and after implantation.

Twenty kidney tumors were transplanted into mice. Successful tumor growth was detected in 19 cases (95%). The histopathologic and immunophenotypic features of the xenografts and those of the original tumors largely overlapped in all the cases. Evaluation of genetic alterations in a subset of 10 cases demonstrated that the grafts largely retained the genetic features of the pre-implantation RCC tissues. Indeed, primary tumors and corresponding grafts displayed identical *VHL* mutations. Moreover, an identical pattern of DNA copy amplification or loss was observed in 6 of 10 cases (60%).

In summary, orthotopic engrafting of RCC tissue fragments can be successfully used to generate animal models that closely resemble RCC in patients. These models will be invaluable for *in vivo* preclinical drug testing, and for deeper understanding of kidney carcinogenesis.

Correspondence, proofs, and request for reprints, to Sabina Signoretti, M.D., Department of Pathology, Brigham and Women's Hospital, Harvard Medical School, 75 Francis Street; Boston; Massachusetts 0215 USA; Tel.: 617-525-7437; Fax: 617-264-5169; ssignoretti@partners.org.

The authors declare no conflict of interest.

The raw data of the SNP array analysis is in the process of being deposited in the GEO database.

Statement of author contributions

SS and CG conceived the experiments. CG, AS, MC, and AP carried out experiments. CG, ADN, RB and SS analyzed the data. CG and SCC performed the statistical analysis. CG and SS wrote the paper and all authors approved the version submitted for publication.

Keywords

Renal Cell Carcinoma; mouse model; orthotopic xenograft; sub-renal capsule implantation

Introduction

Renal Cell Carcinoma (RCC) is a very aggressive disease that accounts for about 2% of all malignancies (1), with approximately 57,000 new cases and 13,000 deaths in United States in 2009 (2). Unfortunately, the incidence and mortality rate of RCC have increased substantially over previous decades (3–6). While significant advances have been made in the management of RCC over the past few years, systemic treatment for patients with locally advanced or metastatic disease remains suboptimal (7–14). Indeed, VEGF-targeted anti-angiogenic therapies (sunitinib, sorafenib, pazopanib, and bevacizumab) have recently been approved and all produce tumor shrinkage in the majority of patients and significantly prolong median progression free survival. Other treatments targeting the m-TOR pathway (Temsirolimus, Everolimus) offer some benefit although the mechanism of this effect is still being debated (8, 12–14). Unfortunately, responses to these therapies are transient and incomplete, with the vast majority of patients still dying of disease at a median of < 2 years (1, 7, 11). Therefore, there is a great need for novel, more effective treatments.

RCC is a heterogeneous neoplasm that consists of several histological subtypes including clear cell (∼75%), papillary (∼12%), chromophobe (∼4%), collecting duct (∼1%), and unclassified (∼4%) carcinoma (1, 15–17). Mouse models of cancer are critical for improving the understanding of tumor biology, developing biomarkers for early detection and accelerating the identification of novel therapeutic targets. Unfortunately, there are still few animal models that can mimic human RCC (18–21). Despite their invaluable significance to study the genetic mechanisms at the basis of RCC development, these models represent types of kidney tumors (chromophobe RCC and oncocytoma) that account for only a limited number of cases in humans. Currently available models of RCC are mostly based on the orthotopic or subcutaneous implantation of human RCC cell lines in immunodeficient recipient mice (22–25). One main disadvantage of developing cancer models by implanting cell lines is that cancer cells continuously cultured *in vitro* are known to acquire many genetic alterations not found in the original tumor (26). Moreover, due to the limited number of RCC lines, cell line-based models lack the heterogeneity that characterizes kidney cancer in the human population. Studies performed in other organs support the hypothesis that the implantation of intact cancer tissues more accurately represents the human disease (27–30). Specifically, this strategy allows maintaining the critical interactions between cancer cells and their surrounding microenvironment and favors metastasis formation. Of note, recent studies seem to indicate that intact human RCC fragments implanted in mice can successfully grow (27, 31, 32).

Here we describe the development of a panel of well-characterized xenografts of RCC, obtained by implanting intact human cancer tissues orthotopically in immunodeficient recipient mice. To clarify the extent to which these xenografts resemble the corresponding RCCs in the patients, we conducted histological, immunohistochemical and genetic evaluations of the original tumor samples and the matched first passage xenografts. Results show that our mouse models closely mimic human RCC, thus providing valuable opportunities for deeper understanding of kidney carcinogenesis and for preclinical and translational applications.

Materials and Methods

Ethics Statement

De-identified human kidney tumor samples were obtained from radical or partial nephrectomies performed at the Brigham and Women's Hospital and the Beth Israel Deaconess Medical Center (Boston, MA, USA). All patients provided written informed consent according to a protocol approved by the Institutional Review Boards of the Dana-Farber Cancer Institute (DFCI Legacy # 01-130). This study was also specifically approved by the IRB of the Dana-Farber Cancer Institute (DFCI Legacy # 06-039) (Table 1). Animal care and experiments were performed in accordance with the guidelines of the Harvard Medical Area Standing Committee on Animals and this Committee specifically approved this study (protocol # 04211).

Primary Kidney Tumor Tissue Samples

Viable tumor tissue was harvested from a single tumor area within 60 minutes from surgical removal and preserved in Dulbecco's Modified Eagle Medium (Invitrogen) containing 10% fetal bovine serum, penicillin and streptomycin (100mg/ml each; Invitrogen) on ice. Each tissue sample was divided into two parts. One part was frozen and evaluated to confirm histological features and rule out the presence of significant hemorrhagic/necrotic areas, not suitable for experimentation. The remaining part was cut into multiple fragments ($\sim 1mm^3$) and used for implantation.

Transplantation experiments

Recipient immunodeficient mice (NOD/SCID, Jackson Laboratories, Bar Harbor, Maine and Nu/Nu, Charles River, Wilmington, MA) were anesthetized with ketamine (100 mg/kg i.p.) and xylazine (10 mg/kg i.p.). Using sterile surgical techniques, tissue fragments from 20 renal tumors were selected as described above and engrafted under the kidney capsule of forty-seven recipient mice (total volume $\sim$ 3–20 mm^3 per kidney) (Supplementary Table 1). Tissue fragments from a subset of 8 tumors were also implanted subcutaneously in eight mice.

Two to twelve months after implantation, mice were euthanized and xenografts were fixed in 10% formalin and embedded in paraffin. For a subset of 10 cases, xenograft tissues were also embedded in optimal cutting temperature (OCT) medium and frozen at −80°C for genetic studies. Since the shape of the xenografts approximated that of a half cylinder, xenograft volumes were estimated using the equation for the volume of a half cylinder ($\pi r^2 h/2$) (33).

Immunohistochemical staining

Immunohistochemical analysis was performed in one randomly selected xenograft per case. Five μm-thick tissue sections of primary tumor samples and matched grafts were immunostained using the EnVision™+ System horseradish peroxidase detection kit (Dako). Briefly, sections were deparaffinized and rehydrated in water, and antigen retrieval was done by heating slides in citrate buffer (pH 6.0) for CAIX, CD34 and CD45 or EDTA buffer (pH 8.0) for Ki67, CD10, and VEGF in a pressure cooker for 2 minutes. Sections were blocked with Peroxide Block (Dako) for 5 minutes and incubated with mouse-anti-human CAIX (1:15000, clone M75), mouse-anti-human Ki67 (1:100, Dako), rat-anti-mouse CD34 (1:100, Abcam), mouse-anti-human CD34 (ready to use, Immunotech), mouse-anti-human CD45 (1:25, Dako), rat anti-mouse CD45 (1:25, BD Pharmigen), mouse-anti-human CD10 (1:10, Leica/Novocastra) or rabbit-anti-human VEGF (C-term) (1:100, Epitomics) antibody for 1 hour at room temperature. Sections were washed for 5 minutes in PBS and incubated with the anti-mouse HRP-conjugated antibody for 30 minutes. Sections were incubated with

the DAB chromogen (Dako) for 5 minutes and lightly counterstained with hematoxilin. For human CD34 and human CD45 staining, tissue sections were incubated with the Mouse on Mouse Blocking Reagent (Vector Laboratories) for 1 hour prior to incubation with the primary antibody. Substitution of the primary antibody with phosphate buffered saline (PBS) served as negative staining control.

Histopathological evaluation and immunohistochemical scoring

Light microscopy evaluation of H&E-stained sections and immunostained slides was performed by two independent pathologists (SS and ADN). For CD34 and CD45 stains, the presence of human-derived and/or mouse-derived CD34-positive or CD-45-positive cells was recorded. Ki67 stain was scored by determining the percentage of tumor cells displaying nuclear staining in 10 randomly selected high-power fields (40X). Semi-quantitative analysis of CAIX, CD10, and VEGF stains was performed by estimating the percentage of tumor cells displaying membrane (CAIX and CD10) or cytoplasmic (VEGF) staining. For all biomarkers, the intensity of expression was classified as weak (1+), moderate (2+), or strong (3+). In cases characterized by heterogeneous expression levels, the two predominant expression intensities were reported.

Expression levels of the markers were considered to be concordant in the original tumor and matched xenograft if results of the immunohistochemical scoring in the two samples showed a difference within +/− 10%.

Genetic analyses

To ensure at least 70% contribution from tumor cells, enriched tumor areas were isolated from 7 μm-thick tissue frozen sections using a fine needle with the aid of an optical microscope. DNA was then extracted using phenol chloroform (26).

Von Hippel-Lindau gene (*VHL*) mutational analysis was performed by direct sequencing. as previously described (26). For DNA copy number analysis, the Sty I (250K) SNP array of the 500K Human Mapping Array (Affymetrix) was used. Arrays were scanned by GeneChip Scanner 3000 7G. Probe-level signal intensities were normalized to a baseline array with median intensity using invariant set normalization and SNP-level signal intensities were obtained using a model-based (PM/MM) method, as previously described (26). All SNP array data are available through the Gene Expression Omnibus database.

Results

Orthotopic RCC grafts are recovered at high efficiency

Fresh tumor tissue from 20 kidney tumors, including 17 clear cell RCC (cRCC), 2 papillary RCC (pRCC), and 1 oncocytoma, was obtained from patients who underwent either partial or radical nephrectomy. Five cRCCs had Fuhrman's nuclear grade (FNG) 2, 8 cRCCs and 2 pRCC s had FNG 3, and 3 cRCCs had FNG 4. Most patients were males (65%) and their ages ranged between 18 and 83 years (Table 1).

For all but one of the 20 transplanted cases (95%), we observed successful tumor growth in at least one transplantation site. The one tumor that completely failed to grow was a transplanted cRCC. Overall, tumor growth was detected in 40 of 47 (85%) of engrafted sites and the volume of the grafts ranged from 2.4 to 29,452.5 mm^3 (Figure 1A and Supplementary Table 1). In most cases the tumor presented a circumscribed growth pattern and did not invade the renal parenchyma of the mouse host. However, in two cRCC cases (cases # 3 and 6) the tumor grossly infiltrated both the renal parenchyma and neighboring organs (e.g. liver and spleen) (not shown).

We chose to implant tumor tissue under the renal capsule because this site is highly vascularized, and, importantly, closely mimics the original microenvironment (27, 29, 34–36). However, monitoring of graft growth at the orthotopic site (i.e. kidney) requires imaging techniques, which are not readily available. Therefore, in the attempt to develop tumor models that can be more easily monitored, 8 of the 20 RCC cases were also grafted subcutaneously. We found that the recovery rate of the subcutaneous grafts was relatively low (2/8 grafts, i.e. 25%).

Orthotopic RCC grafts have morphologic and phenotypic features comparable to those of the original human tumors

We first analyzed the pre- and post-implantation tumor tissues by light microscopy. Specifically, pathologic features including histologic subtype, FNG, pattern of growth (i.e. alveolar, papillary, solid, tubular alveolar) and cytological characteristics (i.e. clear or granular) were evaluated and compared in the primary tumors and corresponding xenografts at the primary passage.

All tumors that successfully grew in the animal host exhibited the same pathological characteristics of the original human tumors (Table 1; Figure 1B). Two cRCC cases were characterized by the presence of extensive hemorrhagic areas in the pre-implantation tissue. Of note, similar hemorrhagic features were also found in the corresponding grafts (not shown).

The proliferation index of the neoplastic cells was also concordant in all the pre and post-transplantation tissues (Figure 2A and Supplementary Table 2). This proliferation index was assessed by Ki67 immunohistochemistry (37). Nuclear positivity for Ki67 varied between 3% and 70%. Of note, all grafts were characterized by the presence of proliferating tumor cells, indicating actual tumor growth in the host.

The immunophenotypical characteristics of the xenografts were also similar to those of the original tumors. We evaluated molecular markers expressed by RCC and utilized in pathological evaluation of renal tumors, including Carbonic Anhydrase IX (CAIX), and CD10 (38–41). In addition, VEGF levels were also investigated. Results are summarized in Supplementary Table 2 and representative immunostains of primary tumors and corresponding grafts are shown in Figure 2A. The original tumors exhibited expression of CAIX, a molecular marker of cRCC (42, 43), in 16 cases (84.2%), including 15 of 16 clear cell carcinoma cases. The percentage of positive cells ranged from 50 to 100%. CD10 immunoreactivity, was observed in 18 primary tumors (94.7%), with a percentage of positive cells that ranged between 2 to 90%. VEGF expression was detected in all primary tumors, with a percentage of positive cells that ranged from 1 to 95%. Of note, in almost all cases (18 of 19) concordant levels of CAIX were observed in the original human tumors and the corresponding grafts. CD10 expression was found to be concordant in 13 of 19 cases (68.4%), and VEGF levels were concordant in 10 of 19 cases (52.6%). For all molecular markers, the majority of cases with concordant proportions of positive cells in the tumors and matching grafts also displayed concordant staining intensity (Supplementary Table 2).

Orthotopic RCC grafts retain the genetic characteristics of the original human tumors

We further investigated whether genetic alterations were similar in the human RCC samples and the corresponding grafts at the primary passage. Since 60–80% of sporadic cRCCs harbor mutations in *VHL* (1, 44), we performed *VHL* mutational analysis in a subset of 10 cases for which frozen tissue was available (9 cRCC and 1 pRCC). Importantly, a genome-wide analysis of copy number changes was also conducted on the same subset of cases. By direct sequencing, we detected *VHL* mutations of in 7/9 (78%) cRCC cases analyzed. As

expected, no *VHL* mutations were observed in the pRCC case. Of note, for all cases, identical mutations were found in the original RCC tissues and the corresponding grafts (Table 2). Since it has been suggested that *VHL* mutations might have prognostic value in patients with cRCC (45), we investigated the relation between *VHL* mutations and tumor growth. There was no significant association between *VHL* mutational status and the average graft volume (exact Wilcoxon-Mann-Whitney test, $p = 1$)

Genome-wide analysis of copy number changes in pre- and post-implantation tissues was performed using high-density single nucleotide polymorphism (SNP) arrays. Several genetic abnormalities have been previously described in RCC and a systematic genomic analysis of cRCC from our group recently identified 14 regions of nonrandom copy-number change, including 7 regions of amplification (1q, 2q, 5q, 7q, 8q, 12p, and 20q) and 7 regions of deletion (1p, 3p, 4q, 6q, 8p, 9p, and 14q) (26, 46–48).

We first assessed the presence of such non-random alterations in the original human tumors. As expected, all 14 non-random alterations were detected in our data set (Figure 3 and Supplementary Table 3). In line with our previously published data, we found that the most frequent copy number events were chromosome (chr) 3p deletion (90%) and chromosome 5q amplification (60%).

We then compared the copy number profiles of the original tumors to those of the corresponding xenografts (Figure 3). In 6 of 10 cases (60%), the grafts displayed a profile of copy number changes identical to those of the pre-implantation tissues. In two cases, the grafts showed the presence of several chromosomal abnormalities not detected in the original tumors. These abnormalities included amplification at chromosome 3q, 4p, 8q, and 16p and deletion of chromosomes 4q, 8p, 9, 11q, 14, 16q, and 18 in one case (#6), and amplification of chromosome 19 and 20 and deletion of chromosomes 4q, 6q, 9, 10 and 15p in the other case (#12). In the remaining two cases, the grafts did not a single genetic alteration observed in the original tumors. Such alteration consisted of chromosome 1q amplification in one case (#3) and amplification of portion of chromosome 5p in the other case (#19). Of note, we found a positive association between the number of non-random genetic changes in the grafts and the average graft volume (exact Spearman's correlation test, $p = 0.033$).

Orthotopic RCC grafts develop metastases

We observed that two orthotopically implantated cRCC tumors consistently invaded the kidney parenchyma and spread to the neighboring organs. One of these two xenografts (case #3) also caused distant metastatic disease in the recipient animals (Figure 4), which were sacrificed only 2 months after transplantation because of shallow breathing. Pathological examination indicated extensive infiltration of abdominal organs (Figure 4B) as well as the presence of multiple metastatic nodules in the lungs (Figure 4A). Remarkably, review of clinical data revealed that the patient had rapidly developed widespread metastatic disease and had died a few months after surgery. The other engrafted RCC case (# 1) known to have caused metastases in the patient (Table 1), however, did not grow in the mouse host.

There was no significant association between the grade of the human RCC and the aggressiveness (i.e. local invasion and/or metastases) of the corresponding xenografts (Fisher's exact test, $p = 0.38$).

A subset of orthotopic RCC grafts contain blood vessels lined by human endothelial cells

Since xenografts were developed by implanting intact human tumor tissue fragments, we investigated whether the endothelial cell component of the vasculature had been replaced

over time by murine cells by assessing the expression of species-specific CD34, a well-known marker of endothelial cells (49).

Ten cases (9 cRCC and 1 pRCC) were characterized by absence of human vasculature and presence of solely murine endothelial cells lining the blood vessel. In the remaining 9 cases (7 cRCC, 1 oncocytoma and 1 pRCC), however, blood vessels of human origin were detected in addition to blood vessels lined by murine endothelial cells. In these cases, the newly generated murine vasculature progressively infiltrated the graft starting from the periphery, enclosing a central area containing the human vasculature (Supplementary Table 2 and Figure 2B). We found a significant association between the persistence of human vessels and the xenograft volume. Indeed, residual human vasculature was observed in 9 of 13 cases (69%) with tumor volume below 200 mm^3, but in none of the six cases with tumor volume higher than 200 mm^3 (Fisher's exact test; $p = 0.01$). The presence of human-derived endothelial cells was also positively associated with the percentage of VEGF-positive tumors cells in the grafts (exact Wilcoxon-Mann-Whitney test, $p = 0.005$), but it was not significantly associated with VEGF staining intensity (exact Wilcoxon-Mann-Whitney test, $p = 0.30$). There was no significant association between the persistence of human vessels and proliferation index (Fisher's exact test, $p = 0.1$), Fuhrman nuclear grade (Fisher's exact test, $p = 0.6$), or time of growth in the host (Fisher's exact test, $p = 0.2$).

We also investigated the presence of cells of hematopoietic origin in the xenografts by assessing the expression of species-specific CD45 (leukocyte common antigen). We observed rare murine CD45-positive cells, mostly within blood vessels. Sparse human-derived CD45-positive cells infiltrating tumor nests were detected in 4/14 (29%) xenografts (Supplementary Figure 1).

Discussion

With this study we propose a method for developing clinically significant animal models of RCC, which could be very useful for clarifying numerous aspects of RCC tumorigenesis and for accelerating the development of novel targeted treatments.

Compared with RCC xenograft models based on the implantation of tumor cell suspensions, our study introduces a means to more closely mimic the biological characteristics of the human disease. Indeed, the orthotopic implantation of the intact fragments of human RCC allows at all times the preservation of cell-to-cell and cell-to-matrix interactions present in the original tumor, which are known to play a key role in tumor growth (27, 29, 34–36). Our high rate of graft success (i.e. 95%) strongly supports this concept. As opposed to the orthotopic implantation, however, and in line with reports from other groups (30, 31, 36, 50, 51), we observed that the recovery rate of the subcutaneously grafted RCCs was relatively low (25%). These findings can be partially explained by the significantly higher levels of vascularization of this site relative to the subcutaneous compartment. Furthermore, it is likely that by more closely mimicking the complex molecular milieu in which the tumor originated, the kidney microenvironment facilitates the survival and proliferation of the cancer cells in the mouse host.

We detected a considerable variability of the xenografts growth rate, with a few of them growing very little or regressing. Of note, such variability was observed even among xenografts generated from the same tumor. It is well recognized that human kidney tumors are very heterogeneous in their composition and that even adjacent regions of the same neoplastic lesion contain highly variable proportions of tumor, stromal, and inflammatory cells as well as variable amounts of necrosis. Although, we performed histopathological analysis to try and identify tumor areas optimal for transplantation, and transplanted similar

amounts of tissue (minimally for each case), it is likely that the amount of viable tumor cells implanted in each kidney was highly variable. It is, therefore, reasonable to hypothesize that engrafted tissues with a small number (or absence) of viable tumor cells grew very little or regressed. However, additional factors including technical issues and differential ability of tumor cell subsets to survive in the mouse microenvironment might have also played a role.

The development of more effective therapies for RCC would greatly benefit from the availability of animal models that represent the phenotypic and genetic heterogeneity of RCC tumors in the human population. Cancer xenograft models have been extensively utilized in preclinical studies of anti-cancer drug activity with variable success (52, 53). While xenografts derived from human cell lines are often of limited use for predicting responses to anti-cancer therapy in humans (52, 54), it has been suggested that orthotopic xenografts derived from primary tumors might be of value for this purpose (52, 55, 56). However, the extent to which orthotopic xenograft models actually resemble human primary tumors has been rarely investigated (31, 57) and extensive validation studies are required before orthotopic RCC models are widely implemented in the preclinical setting.

Our study demonstrates high levels of histological, immunophenotypical and genetic concordance between our orthotopic RCC xenografts and the corresponding primary tumors. Remarkably, overlapping histopathologic features and identical *VHL* mutations were observed in the pre-implantation tumors and the corresponding xenografts at the first passage. Moreover, by genome-wide DNA copy number analysis, six of ten cases displayed the same genetic alterations. In two cases, a single genetic abnormality was observed in the primary tumor but not in the matched xenograft. In the two remaining cases, the copy number profiles of the pre- and post-implantation tissues were considerably discordant with several genetic alterations detected in xenografts but not in the original tumors. The acquisition of new genetic changes leading to growth advantage of selected cell subpopulation(s) within the graft could account for some of these findings. However, heterogeneity of genetic alterations in different regions of the primary tumors might also play a key role, especially in explaining genetic abnormalities present in the original tumor but not in the matched graft (58–60). Indeed, the genetic heterogeneity of the neoplastic cells implanted in the murine host might have led to selection of tumor cell subclone(s) that more rapidly adapted to survive and/or grow in the host environment. In alternative, it is also possible that the dissection of genetically heterogeneous tumors could have caused random selection of subclone(s) of tumor cells prior to implantation in the host. Further genomic analyses of larger series of pre-and post-implantation tumor tissues as well as functional studies are needed to clarify whether any of the genetic alterations detected in the xenografts but not in the corresponding primary tumors play a functional role in tumor growth and progression in RCC.

The survival of patients with kidney cancer is unfortunately still limited by the development of metastases, which occur in a significant proportion of cases (i.e. ~ 30%) (1, 4, 61). For this reason, major effort has been placed in generating tumor models to study human renal cancer growth and progression *in vivo*, especially metastasis development. Of note, two of our xenograft tumors invaded contiguous organs. In addition, one of two RCC cases known to have caused metastases in patients also produced multiple lung metastases.in the murine hosts. These data indicates that at least a subset of our orthotopic RCC xenograft models has the potential to reproduce metastatic patterns of human cancer *in vivo* and could be useful to investigate genetic and epigenetic events that dictate RCC cell dissemination, and to potentially develop novel therapeutic treatments.

In conclusion, we demonstrate the orthotopic engrafting of RCC tissue fragments can be successfully used to generate animal models that closely resemble RCC in patients. Future

studies are needed to determine whether xenografts serially transplanted in the mouse host continue to retain features of the primary human tumors. The development of stable models that can be successfully passaged in mice and are readily available for pre-clinical studies would certainly represent a further improvement over the first passage xenografts described in this paper.

Supplementary Material

Refer to Web version on PubMed Central for supplementary material.

Acknowledgments

We thank Victoria E. Brown and Brittany Bahamon for assistance with immunohistochemical stains.

This work was supported by the Dana-Farber/Harvard Cancer Center Kidney Cancer SPORE and by an Award from Istituto Dermopatico dell'Immacolata, Italy to S.S·· C.G. is recipient of an American-Italian Cancer Foundation's International Post-Doctoral Research Fellowship·· A.D.N. is recipient of a Fellowship Award from the Achille Lattuca Foundation, Italy. R.B. is recipient of awards from the NIH (K08CA122833) and the Doris Duke Charitable Foundation.

References

1. Cohen HT, McGovern FJ. Renal-cell carcinoma. N Engl J Med. 2005 Dec 8; 353(23):2477–2490. [PubMed: 16339096]
2. Jemal A, Siegel R, Ward E, Hao Y, Xu J, Thun MJ. Cancer statistics, 2009. CA Cancer J Clin. 2009 Jul-Aug;59(4):225–249. [PubMed: 19474385]
3. McLaughlin JK, Lipworth L, Tarone RE. Epidemiologic aspects of renal cell carcinoma. Semin Oncol. 2006 Oct; 33(5):527–533. [PubMed: 17045081]
4. Rini BI, Campbell SC, Escudier B. Renal cell carcinoma. Lancet. 2009 Mar 28; 373(9669):1119–1132. [PubMed: 19269025]
5. Hollingsworth JM, Miller DC, Daignault S, Hollenbeck BK. Rising incidence of small renal masses: a need to reassess treatment effect. J Natl Cancer Inst. 2006 Sep 20; 98(18):1331–1334. [PubMed: 16985252]
6. Hollingsworth JM, Miller DC, Daignault S, Hollenbeck BK. Five-year survival after surgical treatment for kidney cancer: a population-based competing risk analysis. Cancer. 2007 May 1; 109(9):1763–1768. [PubMed: 17351954]
7. Yagoda A, Abi-Rached B, Petrylak D. Chemotherapy for advanced renal-cell carcinoma: 1983–1993. Semin Oncol. 1995 Feb; 22(1):42–60. [PubMed: 7855619]
8. Motzer RJ, Russo P. Systemic therapy for renal cell carcinoma. J Urol. 2000 Feb; 163(2):408–417. [PubMed: 10647643]
9. Cho D, Signoretti S, Regan M, Mier JW, Atkins MB. The role of mammalian target of rapamycin inhibitors in the treatment of advanced renal cancer. Clin Cancer Res. 2007 Jan 15; 13(2 Pt 2):758s–763s. [PubMed: 17255306]
10. Kapoor A, Figlin RA. Targeted inhibition of mammalian target of rapamycin for the treatment of advanced renal cell carcinoma. Cancer. 2009 Aug 15; 115(16):3618–3630. [PubMed: 19479976]
11. McDermott DF. Immunotherapy of metastatic renal cell carcinoma. Cancer. 2009 May 15; 115(10 Suppl):2298–2305. [PubMed: 19402060]
12. McDermott DF, Atkins MB. Immunotherapy of metastatic renal cell carcinoma. Cancer J. 2008 Sep-Oct;14(5):320–324. [PubMed: 18836337]
13. McDermott DF, Rini BI. Immunotherapy for metastatic renal cell carcinoma. BJU Int. 2007 May 99.(5 Pt B):1282–1288. [PubMed: 17441925]
14. Rini BI. Vascular endothelial growth factor-targeted therapy in metastatic renal cell carcinoma. Cancer. 2009 May 15; 115(10 Suppl):2306–2312. [PubMed: 19402073]
15. CJ MFaD. WHO International Histological Classification of Tumors. Berlin: Springer; 1998.

16. Motzer RJ, Bander NH, Nanus DM. Renal-cell carcinoma. N Engl J Med. 1996 Sep 19; 335(12): 865–875. [PubMed: 8778606]

17. Schrader AJ, Rauer-Bruening S, Olbert PJ, Hegele A, Rustemeier J, Timmesfeld N, et al. Incidence and long-term prognosis of papillary renal cell carcinoma. J Cancer Res Clin Oncol. 2009 Jun; 135(6):799–805. [PubMed: 19023595]

18. Eker R. Familial renal adenomas in Wistar rats; a preliminary report. Acta Pathol Microbiol Scand. 1954; 34(6):554–562. [PubMed: 13206757]

19. Eker R, Mossige J, Johannessen JV, Aars H. Hereditary renal adenomas and adenocarcinomas in rats. Diagn Histopathol. 1981 Jan-Mar;4(1):99–110. [PubMed: 7249912]

20. Everitt JI, Goldsworthy TL, Wolf DC, Walker CL. Hereditary renal cell carcinoma in the Eker rat: a unique animal model for the study of cancer susceptibility. Toxicol Lett. 1995 Dec.82–83:621–625.

21. Okimoto K, Kouchi M, Kikawa E, Toyosawa K, Koujitani T, Tanaka K, et al. A novel “Nihon” rat model of a Mendelian dominantly inherited renal cell carcinoma. Jpn J Cancer Res. 2000 Nov 91. (11):1096–1099. [PubMed: 11092972]

22. Wilhelm SM, Carter C, Tang L, Wilkie D, McNabola A, Rong H, et al. BAY 43-9006 exhibits broad spectrum oral antitumor activity and targets the RAF/MEK/ERK pathway and receptor tyrosine kinases involved in tumor progression and angiogenesis. Cancer Res. 2004 Oct 1; 64(19): 7099–7109. [PubMed: 15466206]

23. Chang YS, Adnane J, Trail PA, Levy J, Henderson A, Xue D, et al. Sorafenib (BAY 43-9006) inhibits tumor growth and vascularization and induces tumor apoptosis and hypoxia in RCC xenograft models. Cancer Chemother Pharmacol. 2007 Apr; 59(5):561–574. [PubMed: 17160391]

24. Hillman GG, Wang Y, Che M, Raffoul JJ, Yudelev M, Kucuk O, et al. Progression of renal cell carcinoma is inhibited by genistein and radiation in an orthotopic model. BMC Cancer. 2007; 7:4. [PubMed: 17212824]

25. Cho DC, Cohen MB, Panka DJ, Collins M, Ghebremichael M, Atkins MB, et al. The efficacy of the novel dual PI3-kinase/mTOR inhibitor NVP-BEZ235 compared with rapamycin in renal cell carcinoma. Clin Cancer Res. 2010 Jul 15; 16(14):3628–3638. [PubMed: 20606035]

26. Beroukhim R, Brunet JP, Di Napoli A, Mertz KD, Seeley A, Pires MM, et al. Patterns of gene expression and copy-number alterations in von-hippel lindau disease-associated and sporadic clear cell carcinoma of the kidney. Cancer Res. 2009 Jun 1; 69(11):4674–46781. [PubMed: 19470766]

27. An Z, Jiang P, Wang X, Moossa AR, Hoffman RM. Development of a high metastatic orthotopic model of human renal cell carcinoma in nude mice: benefits of fragment implantation compared to cell-suspension injection. Clin Exp Metastasis. 1999 May; 17(3):265–270. [PubMed: 10432012]

28. Gray DR, Huss WJ, Yau JM, Durham LE, Werdin ES, Funkhouser WK Jr, et al. Short-term human prostate primary xenografts: an in vivo model of human prostate cancer vasculature and angiogenesis. Cancer Res. 2004 Mar 1; 64(5):1712–1721. [PubMed: 14996731]

29. Lee CH, Xue H, Sutcliffe M, Gout PW, Huntsman DG, Miller DM, et al. Establishment of subrenal capsule xenografts of primary human ovarian tumors in SCID mice: potential models. Gynecol Oncol. 2005 Jan; 96(1):48–55. [PubMed: 15589579]

30. Wang Y, Revelo MP, Sudilovsky D, Cao M, Chen WG, Goetz L, et al. Development and characterization of efficient xenograft models for benign and malignant human prostate tissue. Prostate. 2005 Jul 1; 64(2):149–159. [PubMed: 15678503]

31. Karam JA, Zhang XY, Tamboli P, Margulis V, Wang H, Abel EJ, et al. Development and Characterization of Clinically Relevant Tumor Models From Patients With Renal Cell Carcinoma. Eur Urol. 2010 Dec 8.

32. Murphy EA, Shields DJ, Stoletov K, Dneprovskaia E, McElroy M, Greenberg JI, et al. Disruption of angiogenesis and tumor growth with an orally active drug that stabilizes the inactive state of PDGFRbeta/B-RAF. Proc Natl Acad Sci U S A. Mar 2; 107(9):4299–4304. [PubMed: 20154271]

33. Weisstein, E. CRC Concise Encyclopedia of Mathematics. 2nd edn. Boca Raton, FL: CRC Press, Inc; 2002.

34. Cui JH, Krueger U, Henne-Bruns D, Kremer B, Kalthoff H. Orthotopic transplantation model of human gastrointestinal cancer and detection of micrometastases. World J Gastroenterol. 2001 Jun; 7(3):381–386. [PubMed: 11819794]

35. Garcia-Olmo D, Garcia-Rivas M, Garcia-Olmo DC, Atienzar M. Orthotopic implantation of colon carcinoma cells provides an experimental model in the rat that replicates the regional spreading pattern of human colorectal cancer. Cancer Lett. 1998 Oct 23; 132(1–2):127–133. [PubMed: 10397463]
36. Yi XF, Yuan ST, Lu LJ, Ding J, Feng YJ. A clinically relevant orthotopic implantation nude mouse model of human epithelial ovarian cancer--based on consecutive observation. Int J Gynecol Cancer. 2005 Sep-Oct;15(5):850–855. [PubMed: 16174235]
37. Aaltomaa S, Lipponen P, Ala-Opas M, Eskelinen M, Syrjanen K. Prognostic value of Ki-67 expression in renal cell carcinomas. Eur Urol. 1997; 31(3):350–355. [PubMed: 9129930]
38. Zhou M, Roma A, Magi-Galluzzi C. The usefulness of immunohistochemical markers in the differential diagnosis of renal neoplasms. Clin Lab Med. 2005 Jun; 25(2):247–257. [PubMed: 15848735]
39. Langner C, Ratschek M, Rehak P, Schips L, Zigeuner R. CD10 is a diagnostic and prognostic marker in renal malignancies. Histopathology. 2004 Nov; 45(5):460–467. [PubMed: 15500649]
40. Allory Y, Bazille C, Vieillefond A, Molinie V, Cochand-Priollet B, Cussenot O, et al. Profiling and classification tree applied to renal epithelial tumours. Histopathology. 2008 Jan; 52(2):158–166. [PubMed: 18036175]
41. Liu L, Qian J, Singh H, Meiers I, Zhou X, Bostwick DG. Immunohistochemical analysis of chromophobe renal cell carcinoma, renal oncocytoma, and clear cell carcinoma: an optimal and practical panel for differential diagnosis. Arch Pathol Lab Med. 2007 Aug; 131(8):1290–1297. [PubMed: 17683191]
42. Bui MH, Seligson D, Han KR, Pantuck AJ, Dorey FJ, Huang Y, et al. Carbonic anhydrase IX is an independent predictor of survival in advanced renal clear cell carcinoma: implications for prognosis and therapy. Clin Cancer Res. 2003 Feb; 9(2):802–811. [PubMed: 12576453]
43. Atkins M, Regan M, McDermott D, Mier J, Stanbridge E, Youmans A, et al. Carbonic anhydrase IX expression predicts outcome of interleukin 2 therapy for renal cancer. Clin Cancer Res. 2005 May 15; 11(10):3714–3721. [PubMed: 15897568]
44. Sudarshan S, Linehan WM. Genetic basis of cancer of the kidney. Semin Oncol. 2006 Oct; 33(5): 544–551. [PubMed: 17045083]
45. Cowey CL, Rathmell WK. VHL gene mutations in renal cell carcinoma: role as a biomarker of disease outcome and drug efficacy. Curr Oncol Rep. 2009 Mar; 11(2):94–101. [PubMed: 19216840]
46. Kovacs G. Molecular cytogenetics of renal cell tumors. Adv Cancer Res. 1993; 62:89–124. [PubMed: 8109322]
47. Thrash-Bingham CA, Greenberg RE, Howard S, Bruzel A, Bremer M, Goll A, et al. Comprehensive allelotyping of human renal cell carcinomas using microsatellite DNA probes. Proc Natl Acad Sci U S A. 1995 Mar 28; 92(7):2854–2858. [PubMed: 7708737]
48. Thrash-Bingham CA, Salazar H, Freed JJ, Greenberg RE, Tartof KD. Genomic alterations and instabilities in renal cell carcinomas and their relationship to tumor pathology. Cancer Res. 1995 Dec 15; 55(24):6189–6195. [PubMed: 8521412]
49. Harraz M, Jiao C, Hanlon HD, Hartley RS, Schatteman GC. CD34- blood-derived human endothelial cell progenitors. Stem Cells. 2001; 19(4):304–312. [PubMed: 11463950]
50. Fidler IJ. Critical factors in the biology of human cancer metastasis: twenty-eighth GHA Clowes memorial award lecture. Cancer Res. 1990 Oct 1; 50(19):6130–6138. [PubMed: 1698118]
51. Togo S, Wang X, Shimada H, Moossa AR, Hoffman RM. Cancer seed and soil can be highly selective: human-patient colon tumor lung metastasis grows in nude mouse lung but not colon or subcutis. Anticancer Res. 1995 May-Jun;15(3):795–798. [PubMed: 7645960]
52. Kerbel RS. Human tumor xenografts as predictive preclinical models for anticancer drug activity in humans: better than commonly perceived-but they can be improved. Cancer Biol Ther. 2003 Jul-Aug;(4 Suppl 1):S134–S139. [PubMed: 14508091]
53. Richmond A, Su Y. Mouse xenograft models vs GEM models for human cancer therapeutics. Dis Model Mech. 2008 Sep-Oct;1(2–3):78–82. [PubMed: 19048064]
54. Killion JJ, Radinsky R, Fidler IJ. Orthotopic models are necessary to predict therapy of transplantable tumors in mice. Cancer Metastasis Rev. 1998; 17(3):279–284. [PubMed: 10352881]

55. Scholz CC, Berger DP, Winterhalter BR, Henss H, Fiebig HH. Correlation of drug response in patients and in the clonogenic assay with solid human tumour xenografts. Eur J Cancer. 1990; 26(8):901–905. [PubMed: 2145936]

56. Johnson JI, Decker S, Zaharevitz D, Rubinstein LV, Venditti JM, Schepartz S, et al. Relationships between drug activity in NCI preclinical in vitro and in vivo models and early clinical trials. Br J Cancer. 2001 May 18; 84(10):1424–1431. [PubMed: 11355958]

57. Priolo C, Agostini M, Vena N, Ligon AH, Fiorentino M, Shin E, et al. Establishment and genomic characterization of mouse xenografts of human primary prostate tumors. Am J Pathol. Apr; 176(4):1901–1913. [PubMed: 20167861]

58. Bissig H, Richter J, Desper R, Meier V, Schraml P, Schaffer AA, et al. Evaluation of the clonal relationship between primary and metastatic renal cell carcinoma by comparative genomic hybridization. Am J Pathol. 1999 Jul; 155(1):267–274. [PubMed: 10393858]

59. Moch H, Schraml P, Bubendorf L, Richter J, Gasser TC, Mihatsch MJ, et al. Intratumoral heterogeneity of von Hippel-Lindau gene deletions in renal cell carcinoma detected by fluorescence in situ hybridization. Cancer Res. 1998 Jun 1; 58(11):2304–2309. [PubMed: 9622063]

60. Jiang F, Moch H, Richter J, Egenter C, Gasser T, Bubendorf L, et al. Comparative genomic hybridization reveals frequent chromosome 13q and 4q losses in renal carcinomas with sarcomatoid transformation. J Pathol. 1998 Aug; 185(4):382–388. [PubMed: 9828836]

61. Bukowski RM. Prognostic factors for survival in metastatic renal cell carcinoma: update 2008. Cancer. 2009 May 15; 115(10 Suppl):2273–2281. [PubMed: 19402065]

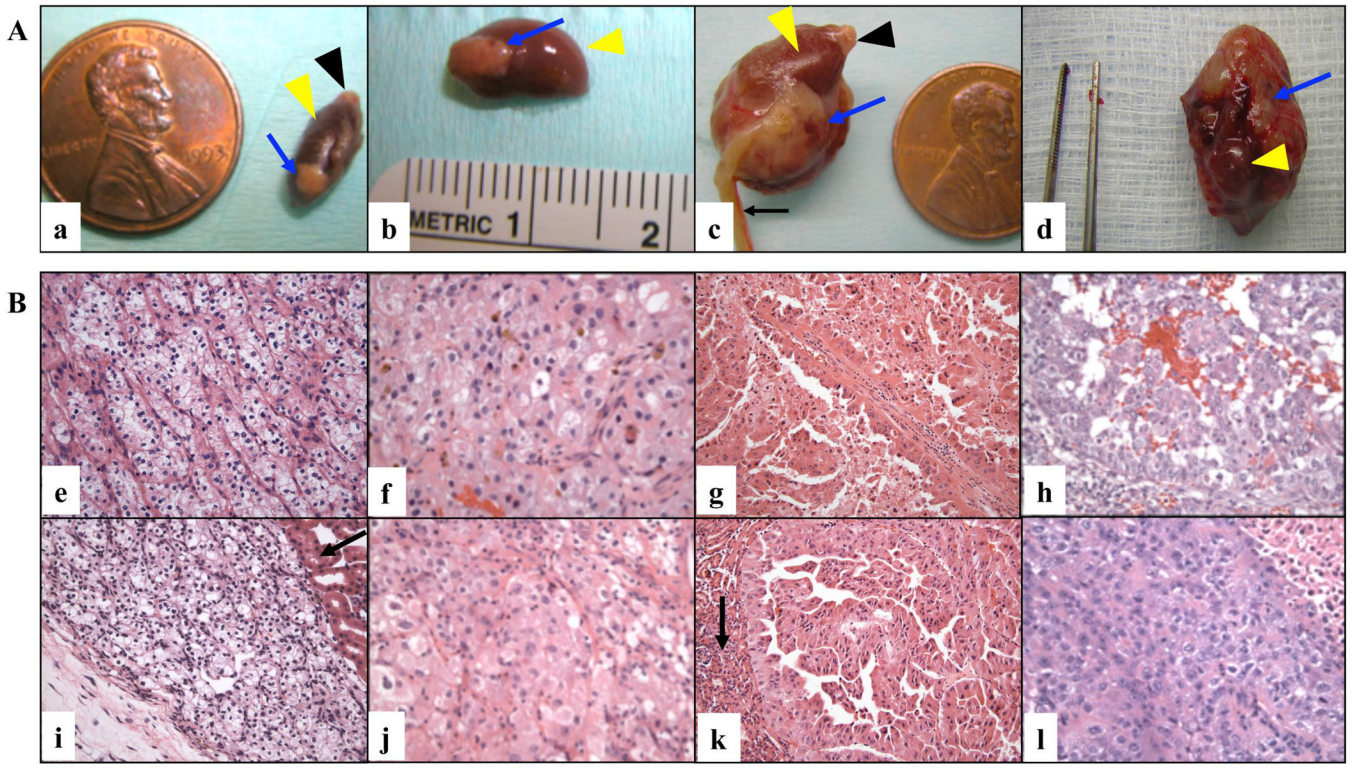

Figure 1. Macroscopic and histological features of RCC grafts

A. Representative gross images of orthotopic RCC grafts (X200 magnification). Examples of three cRCC cases (a, case # 5; c, case # 6; d, case # 3) and one pRCC case (b, case # 11) are shown. Blue arrows indicate the engrafted tumor; yellow arrowheads indicate murine kidney; black arrowheads indicate murine adrenal gland; and the black arrow indicates the uterus of the mouse host. B. Representative histological images of H&E stained slides of primary tumors (upper panels, X200 magnification) and corresponding grafts (lower panels, X200 magnification) are shown: (e, i) FNG 2 cRCC (case # 2); (f, j) FNG 3 cRCC (case # 6); (g, k) FNG 3 pRCC (case # 11); (h, l) FNG 4 cRCC (case # 3). Black arrows indicate the mouse kidney.

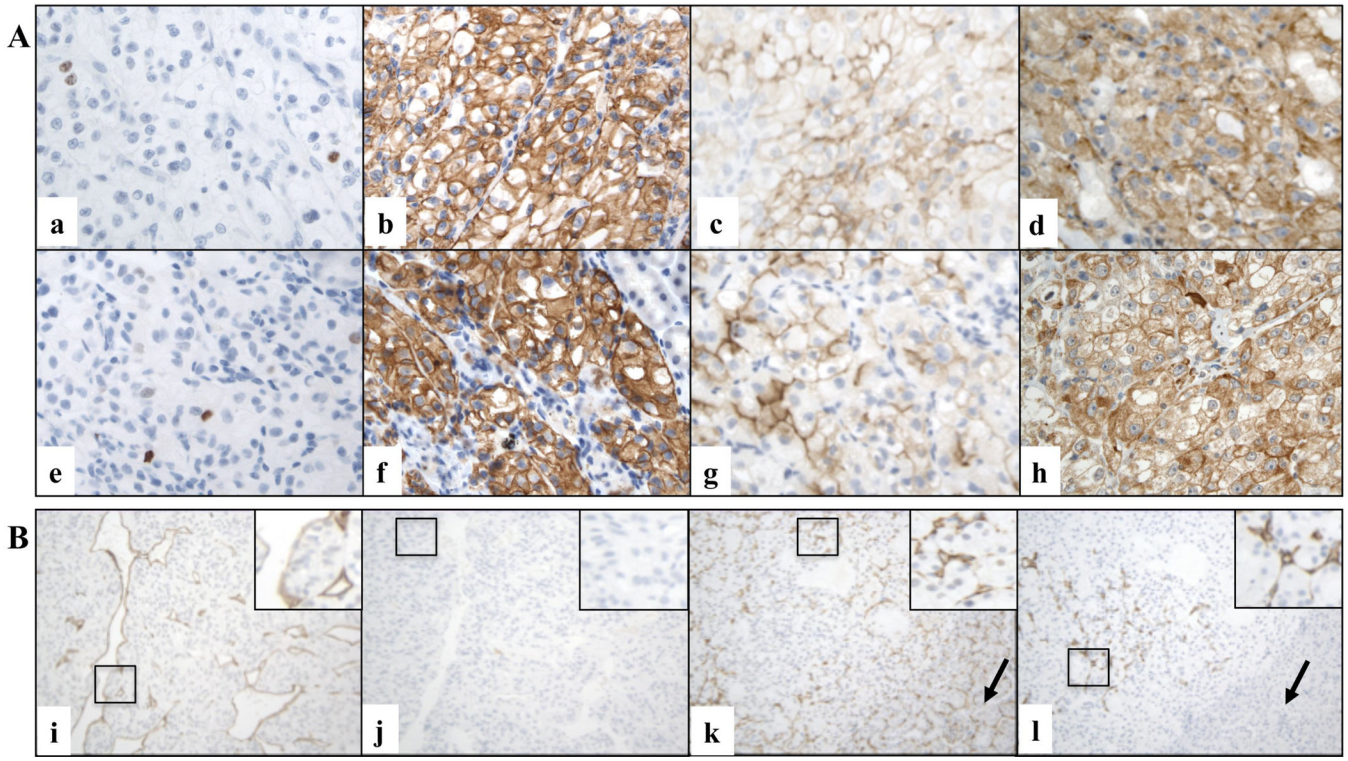

Figure 2. Immunophenotypic characteristics of RCC grafts

A. Representative microscopic images of primary cRCC (a, b, c, d) and matched orthotopic xenograft (e, f, g, h) tissues immunostained for various markers (X600 magnification). Ki67 (a and e, case # 2), CAIX (b and f, case # 2), CD10 (c and g, case # 12), and VEGF (d and h, case # 6) stains are shown. B. Examples of species specific labeling of CD34-positive endothelial cells in two representative xenograft cases (X200 magnification). Murine (i) but not residual human (j) endothelial cells are detected in a FNG 4 cRCC graft grown in the host for 2 months (case # 19). Both murine (k) and human (l) endothelial cells are present in a FNG 3 cRCC graft grown in the host for 8 months (case # 9). Black arrows indicate the kidney of the mouse host.

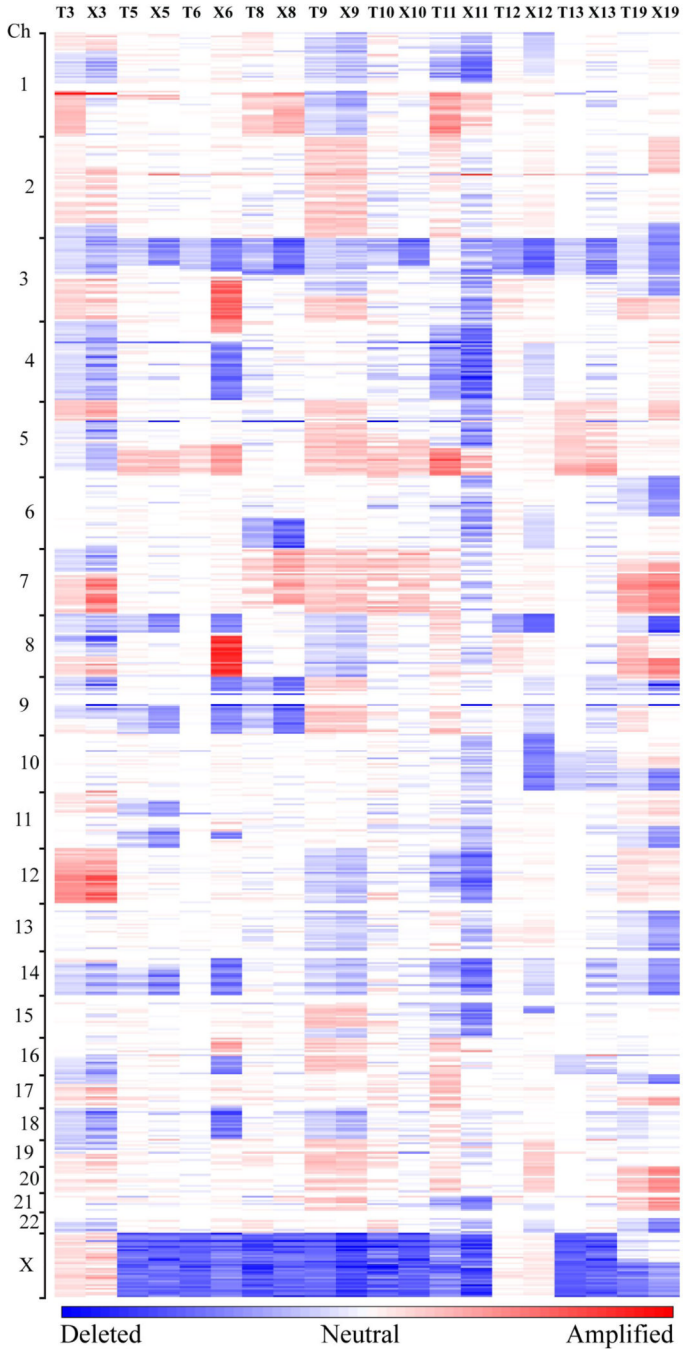

Figure 3. Copy-number profiles of primary RCCs and corresponding xenografts

Amplifications (red) and deletions (blue), determined by normalized signal intensities from 250K SNP arrays are displayed across the genome (chromosomes are indicated along the y axis) for 10 primary RCC cases (T) and the matched xenografts (X). All cases, with the exception of a papillary RCC case (T11/X11), display low signal intensities at chromosome 3p, reflecting copy loss in that region.

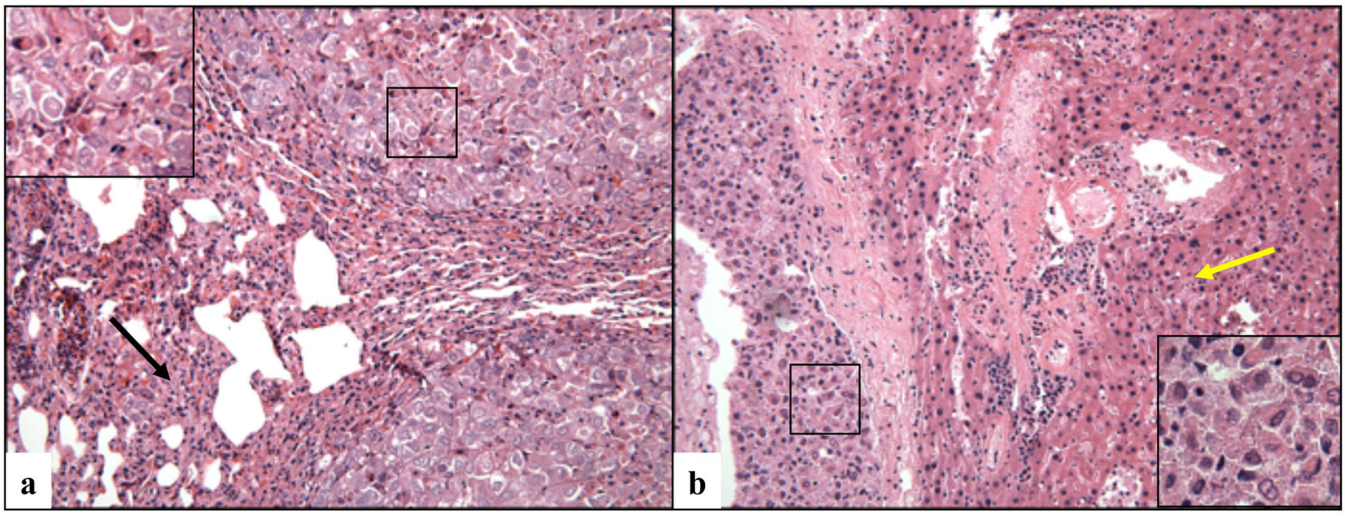

Figure 4. Metastatic spread of ccRCC graft to the host lungs

Microscopic image of metastatic nodules detected in the lung (a) and liver (b) of a mouse that had been carrying an orthotopic cRCC graft (case # 3) for a period of 2.5 months (magnification X200 in the right and left panel, and X400 in the insets). The back arrow indicates the collapsed lung parenchyma surrounding the neoplastic nodule, and yellow arrow indicates the mouse liver.

Table 1

Outline of clinical-pathological characteristics of implanted RCC cases.

Case n.	Age of patient	Sex	Diagnosis	TNM*	Fuhrman Nuclear Grade
1	48	M	cRCC	T3b-c NX M1	2
2	61	M	cRCC	T1 N0 MX	2
3	61	F	cRCC	T3b NX MX	4
4	79	F	cRCC	T3 N0 MX	3
5	63	M	cRCC	T2 N0 MX	2
6	63	M	cRCC	T3b NX M1	3
7	60	M	cRCC	T2 N0 MX	2
8	49	M	cRCC	T1b NX MX	2
9	74	F	cRCC	T1b NX MX	3
10	50	M	cRCC	T2 N0 MX	3
11	56	M	pRCC	T3a N2 MX	3
12	76	F	cRCC	T3b NX MX	3
13	57	M	cRCC	T1b NX MX	3
14	53	F	Oncocytoma	T1 NX MX	-
15	74	M	cRCC	T1b NX MX	2
16	18	F	pRCC	T3 N2 MX	3
17	48	M	cRCC	T3a N0 MX	3
18	54	F	cRCC	T2 N0 MX	3
19	83	M	cRCC	T3b NX MX	4
20	42	M	cRCC	T2 N0 MX	2

*TNM (AJCC Classification 6th edition).

Table 2

Results of VHL mutation analysis in original tumors and corresponding xenografts.

Case n.	Histologica Diagnosis	Tissue type	VHL Mutation	Exon	Mutation Type	Codon and predicted aa change*
3	cRCC	Original	Yes	1	FS	N67fsX158
		Xenograft	Yes	1	FS	N67fsX158
5	cRCC	Original	Yes	1	MS	V74G
		Xenograft	Yes	1	MS	V74G
6	cRCC	Original	Yes	1	NS & MS	S65X & R64S
		Xenograft	Yes	1	NS & MS	S65X & R64S
8	cRCC	Original	Yes	3	MS	L158R
		Xenograft	Yes	3	MS	L158R
9	cRCC	Original	Yes	2	FS	F136fsX158
		Xenograft	Yes	2	FS	F136fsX158
10	cRCC	Original	No	-	-	-
		Xenograft	No	-	-	-
11	pRCC	Original	No	-	-	-
		Xenograft	No	-	-	-
12	cRCC	Original	Yes	3	FS	L158fsX169
		Xenograft	Yes	3	FS	L158fsX169
13	cRCC	Original	Yes	2	FS	L135fsX158
		Xenograft	Yes	2	FS	L135fsX158
19	cRCC	Original	No	-	-	-
		Xenograft	No	-	-	-

* aa: aminoacids

J Pathol. Author manuscript; available in PMC 2013 October 09.